Advances in Engineering Software 185 (2023) 103515

Contents lists available at ScienceDirect

Advances in Engineering Software

journal homepage: www.elsevier.com/locate/advengsoft

Metamodel-assisted hybrid optimization strategy for model updating using vibration response data

Li YiFei [a,b], Cao MaoSen [b,*], Tran N. Hoa [c], S. Khatir [a], Hoang-Le Minh [d], Thanh SangTo [d], Thanh Cuong-Le [d], Magd Abdel Wahab [a,*]

[a] Soete Laboratory, Department of Electrical Energy, Metals, Mechanical Constructions, and Systems, Faculty of Engineering and Architecture, Ghent University, Gent, Belgium
[b] Department of Engineering Mechanics, Hohai University, Nanjing, PR China
[c] Department of Bridge and Tunnel Engineering, Faculty of Civil Engineering, University of Transport and Communications, Hanoi, Vietnam
[d] Center for Engineering Application & Technology Solutions, Ho Chi Minh City Open University, Ho Chi Minh City, Vietnam

ARTICLE INFO

Keywords:
Metamodel
Hybrid optimization strategy
Dynamic parameter identification
Probabilistic finite element analysis
Vibration response

ABSTRACT

In this study, an effective and novel method, termed **M**etamodel **A**ssisted **H**ybrid of **P**article **S**warm **O**ptimization with **G**enetic **A**lgorithm (MA-HPSOGA), is developed to identify unknown structural dynamic parameters. The method first constructs four popular metamodels to substitute the computationally expensive numerical analysis based on the Latin hypercube sampling method and probabilistic finite element analysis, and their accuracy is assessed by R-squared. Subsequently, a suitable and low-cost metamodel is selected in combination with a hybrid optimization strategy by incorporating Genetic Algorithm (GA) into Particle Swarm Optimization (PSO). Two examples with measured vibration response data and different levels of complexity are used to verify the effectiveness and practicality of the presented method. The results showed that polynomial chaos expansion assisted HPSOGA has the highest computational efficiency and accuracy in the four coupled methods. Besides, compared to the conventional iteration-based dynamic parameter identification methods, the presented method shows an overwhelming advantage in terms of computational efficiency. Furthermore, the performance of HPSOGA is compared with its sub-algorithms, showing that the hybrid strategy offers faster convergence and stronger robustness. Our findings reveal that the MA-HPSOGA may be used as a promising method for achieving high-efficiency model updating in large-scale complex structures.

1. Introduction

A mathematical model is a representation or an abstract interpretation of physical reality that is amenable to analysis and calculation. Numerical simulation allows us to calculate the solutions of these models on a computer, and therefore to simulate physical reality. The Finite Element Method (FEM), as one of the most mainstream methods for numerical simulations, has always played an extraordinarily important role in exploring scientific and engineering problems [1]. For example, during project feasibility studies, Finite Element Analysis (FEA) has been applied to large civil engineering structures to pre-assess structural safety, leading to better construction guidance and risk prevention.

However, the structural finite element (FE) models have inherent and epistemic errors, leading to some deviation between the system response after FEA and the real system response. These errors can be divided into the following three categories: (1) idealistic assumptions made to describe the mechanical behavior of physical structures, (2) inherent errors introduced by numerical methods and (3) typical errors arising from incorrect assumptions regarding model parameters. The first two are related to the mathematical structure of the model, which is hard to eliminate, while the last typical error can be reduced by model updating [2,3].

Model updating is essentially an optimization search process for solving inverse problems, and it can be an important tool for calibrating FE models to mitigate modeling errors [4]. By modifying the modeling parameters of the initial FE model, the discrepancy between the model response and the measured system response is minimized, enabling the behavior of the updated FE model to be as close as possible to the corresponding real structure. Conventional model updating methods is

* Corresponding authors.
E-mail addresses: 20110018@hhu.edu.cn (C. MaoSen), magd.abdelwahab@ugent.be (M. Abdel Wahab).

https://doi.org/10.1016/j.advengsoft.2023.103515
Received 18 January 2023; Received in revised form 21 April 2023; Accepted 13 June 2023
Available online 5 July 2023
0965-9978/© 2023 Elsevier Ltd. All rights reserved.

achieved by a trial-and-error approach and sensitivity analysis approach [5,6], which are often time-consuming and may not be feasible in some cases. In recent years, with the rapid development of modern intelligent algorithms, numerous studies have focused on metaheuristic algorithms for FE model updating.

Tran et al. [7] proposed a hybrid metaheuristic algorithm, which incorporates fully the advantages of Genetic Algorithm (GA) and Improved Cuckoo Search (ICS), and then updated the FE model of a large twin steel truss bridge based on vibration measurement data. Dinh et al. [8] developed a Multi-Objective Cuckoo Search (MOCS) algorithm for optimizing the objective function in finite element model updating, and subsequently implemented the identification of the location and extent of multi-damages in functionally graded material structures. Minh et al. [9] developed a new balance of Cuckoo Search (NB-CS) algorithm for model updating and damage identification of three shell models with different levels of complexity, based on co-simulation with SAP2000 software and MATLAB. Sang et al. [10] proposed a novel stochastic optimization algorithm, namely the Planetary Optimization Algorithm (POA), for predicting horizontal displacements of diaphragm wall in high-rise buildings, and the structural FE model was calibrated based on field monitoring data from the early stages of excavation. Wu et al. [11] proposed an improved Crow Search Algorithm based on Levy Flight (LFCSA) for FE model updating, and the superiority of the proposed algorithm was highlighted in comparison with the standard CSA and the PSO algorithm with Levy Flight (LFPSO).

Although modern intelligent algorithms are widely used for model updating, the updating process requires numerous calls to the structural FE model for iterative optimization. Especially for performing structural dynamics or nonlinear analysis, such crude operations make it extremely inefficient to apply modern intelligent algorithms to complex structures. Fortunately, metamodeling techniques provide a bridge between the two. The technique treats the relationship between inputs and outputs as a 'black box' model, allowing to create a computationally inexpensive mathematical approximation to substitute the expensive FE models without requiring additional information about the system [12]. There are some popular metamodels such as Artificial Neural Network (ANN) [13], Polynomial Chaos Expansion (PCE) [14], Kriging [15] and Support Vector Regression (SVR) [16], etc.

Zhou et al. [17] constructed a Multi-Response Gaussian Process (MRGP) metamodel to substitute the structural FE model, and then adopted PSO and Simulated Annealing Algorithm (SAA) to minimize the discrepancy between the predicted and measured structural frequency responses. Naranjo et al. [18] developed a new efficient collaborative algorithm, which combines Harmony Search and Active-Set Algorithm (HS-ASA) and ANN and Principal Component Analysis (PCA). The proposed algorithm was applied to address the model updating of a real steel footbridge. Wang et al. [19] proposed a multi-scale model updating method, which combined Kriging metamodel with Non-dominated Sorting Genetic Algorithm-II (NSGA-II) for identifying the unknown parameters in transmission tower structures. The results showed that the proposed method could improve the accuracy of the tower in both global and local structural responses. Xia et al. [20] combined Back-Propagation Neural Network (BPNN) with Gaussian-white-noise-Mutation Particle Swarm Optimization (GMPSO), proposing an effective model updating method for complex bridge structures.

Most of the literature mentioned above usually only employs single surrogate model in conjunction with the optimization algorithm for model updating, lacking a comprehensive investigation in the computational accuracy and efficiency of surrogate models applied to parameter identification. As it is well known, no single surrogate model was found to be the most effective for all problems. Hence, four widely popular metamodels, are chosen in this study, namely ANN, PCE, Kriging and SVR, with the view of revealing their differential performance in assisting the same hybrid optimization strategy, attempting to expand the boundaries of the existing literature mostly focusing on single metamodel. This paper aims to provide a promising generic paradigm for the rapid implementation of FE model updating, and its innovations have been integrated as follows:

- The differential performance of several popular metamodelling techniques applied to FE model updating are compared and mechanistic explanation for the differences is provided.
- An easy-to-implement method for identifying structural dynamic parameters is constructed using the common surrogate models and the popular optimization algorithms, breaking through the limitations of conventional methods to quickly determine the parameters.
- Compared with the conventional iteration-based methods, the proposed method achieves a qualitative leap in computational efficiency while improving the computational accuracy.

The rest of this article is structured as follows. Section 2 briefly describes the methodology of the four metamodels and HPSOGA, and Section 3 presents the procedures and evaluation metrics for the MA-HPSOGA method. Next, Sections 4 and 5 use two models with varying complexity, aiming to demonstrate the effectiveness and practicality of the proposed method. Conclusions are given in Section 6 and some detailed results are presented in Appendix A.

2. Theoretical fundamentals

This section will briefly introduce the underlying theory of four popular metamodels and HPSOGA.

2.1. Methodology of metamodels

2.1.1. Artificial neural networks

Assuming that the vector $\boldsymbol{X} = (x_1,x_2,\ldots, x_M)$ represents the set of unknown input parameters, and the corresponding model response output vector is expressed as $\boldsymbol{Y}=(y_1,y_2,\ldots, y_M)$ and the hidden layer has n neurons, Fig. 1 describes the Architecture of the proposed ANN [21].

The input and output of the hidden layer are noted as w_l and v_l, respectively, which can be written in the following form [22,23]:

$$w_l = \sum_{k=1}^{M} \delta_{kl} x_k + \gamma_l, l = 1, 2, \ldots, M; \quad v_l = F(w_l) \tag{1}$$

where δ_{kl} and γ_l refer to the weight coefficients and bias parameters linking the input and hidden layers, x_k is the value of the k^{th} input parameters and $F(\cdot)$ is the activation function.

In addition, the input and output of the output layer are noted as φ and $\boldsymbol{Y}$, and they can be expressed as Eq. 2:

$$\varphi = \sum_{l=1}^{M} \vartheta_l v_l + \tau; \ \boldsymbol{Y} = F(\varphi) \tag{2}$$

where ϑ_l and τ refer to the weight coefficient and bias parameters linking

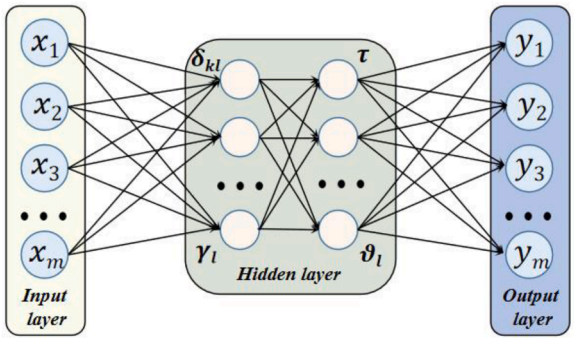

Fig. 1. The Architecture of ANN.

the hidden and output layers.

The output error ε_r for N training data is shown as Eq. 3:

$$\epsilon_r = \sum_{i=1}^{N} \left(p^i - y^i\right)^2 \tag{3}$$

where y^i is the value of the i^{th} model response output, and p^i is the ANN-based predicted output.

The error is propagated backward from the output layer to the hidden layer, and the errors in the output and hidden layers are denoted as $\varepsilon$and α_j, respectively, which can be written as follows:

$$\varepsilon = (p-y)(1-y);\ \ \alpha_j = \varepsilon\vartheta_l(1-Y_l) \tag{4}$$

Hence, the weight coefficient and bias parameters in Eq. 1 and Eq. 2 are calculated as follows:

$$\delta_{kl} = \delta_{kl} + b\alpha_l x_l;\quad \vartheta_l = \vartheta_l + a\varepsilon Y_l$$

$$\gamma_l = \gamma_l + b\alpha_l;\ \ \tau = \tau + a\varepsilon \tag{5}$$

where $0 < a < 1$ is the weight adjustment parameter, $0 < b < 1$ is the learning coefficient.

2.1.2. Polynomial chaos expansion

Polynomial Chaos Expansion (PCE), a powerful metamodeling technique, aims to approximate computational models (e.g., FE models) by constructing spectral representations based on appropriate polynomial functions [14].

Considering a M dimensional unknown input parameters vector $\boldsymbol{X} = \{x_1, x_2, \ldots, x_M\}$ described by the joint PDF $f_{X_k}, k = 1, 2, M$, the output vector Y as a mapping of $\boldsymbol{X}$ with respect to the computational model, denoted $Y = \mathscr{M}(X)$. Y can expressed exactly in an infinite expansion as shown in Eq. (6) [24,25]:

$$Y = \mathscr{M}(\boldsymbol{X}) \approx \mathscr{M}^{PCE}(\boldsymbol{X}) = \sum_{\boldsymbol{w}\in\Omega} \zeta_{\boldsymbol{w}}\delta_{\boldsymbol{w}}(\boldsymbol{X}) \tag{6}$$

where $\boldsymbol{w} = \{w_1, \ldots, w_n\}(w_k \geq 0) \in \Omega$ is the multi-index notation vector and $\Omega \in \mathbb{N}^M$is the truncation set of multi-indices. $\boldsymbol{\zeta} = \{\zeta_1, \ldots, \zeta_n\} \in \mathbb{R}$ is a vector containing the unknown expansion coefficients and $\delta_{\boldsymbol{w}}(\boldsymbol{X}) = \prod_{k=1}^{M} \varphi_{w_k}^{(k)}(x_k)$ are multivariate polynomials orthogonal with respect to $f_{\boldsymbol{X}}$, of which $\varphi_{w_k}^{(k)}$ is the univariate orthogonal polynomial in the k^{th} variable of corresponding index w_k.

In the real world, Eq. (6) usually needs to be truncated to reduce computational costs. There are usually two main truncation options, i.e., standard truncation [26] and hyperbolic truncation [27], the latter serves as an improved modification of the former and is applied in this study, which makes use of the parametric q to define the truncation as below:

$$\Omega^{M,p,q} = \left\{\boldsymbol{w} \in \Omega^{M,p} : \|\boldsymbol{w}\|_q \leq p\right\}, \|\boldsymbol{w}\| = \left(\sum_{i=1}^{M} w_i^q\right)^{\frac{1}{q}}\ card\ \Omega^{M,p} \equiv Q$$
$$= \binom{M+p}{p} = \frac{(M+p)!}{p!M!} \tag{7}$$

where p is the polynomial degree and q is the truncated norm, Q is the total-degree basis, which grows exponentially with the degree p.

In Eq. (7), $q < 1$ corresponds to the hyperbolic truncation scheme, and $q = 1$ is the standard truncation scheme. In general, decreasing the q-value can significantly reduce the number of model evaluations, but some errors may be caused by the absence of higher order terms in high dimensional problems [28]. An easy-to-understand illustration presents varying values of p and q for Hyperbolic truncation [29], and a truncation scheme with $q = 0.75$ is used in this study.

Therefore, the infinite series in Eq. (6) can be rewritten as:

$$Y = \mathscr{M}(\boldsymbol{X}) = \sum_{w=0}^{Q-1} \zeta_{\boldsymbol{w}}\delta_w(\boldsymbol{X}) + \epsilon_p \equiv \boldsymbol{\zeta}^T\delta(\boldsymbol{X}) + \epsilon_p \tag{8}$$

where ε_p is the truncation error, and superscript T means transpose.

Hereafter, it became crucial to calculate the polynomial coefficients, $\boldsymbol{\zeta}$, for constructing the PCE model. Least Angle Regression (LAR) [30] is adapted as a strategy to calculate it, which aims to find coefficient vectors with only a few non-zero solutions, while the other coefficients are set to zero. It can be formulated as follows:

$$\widehat{\boldsymbol{\zeta}} = \underset{\zeta\in\mathbb{R}^P}{arg\ min}\mathbb{E}\left[\left(\boldsymbol{\zeta}^T\delta(\boldsymbol{X}) - Y\right)^2\right] + \lambda\ \|\ \boldsymbol{\zeta}\|_1 \tag{9}$$

where $\|\ \widehat{\boldsymbol{\zeta}}\|_1 = \sum_{\boldsymbol{w}\in\Omega} |\zeta_{\boldsymbol{w}}|$ is the regularization term that forces the minimization to favor low rank solutions.

2.1.3. Kriging

Kriging (or Gaussian process modeling) was first developed as a spatial interpolation tool in Geostatistics in the 1950s [31], until it was introduced to the field of metamodeling in the 1990s by Sacks et al. [32] as an expensive "input-output" mapping relationship for computational models.

Assuming that a Kriging index $\boldsymbol{x} \in \mathscr{D}_X \subset \mathbb{R}^M$ and the model outputs $Y = \mathscr{M}(\boldsymbol{x}) \in \mathbb{R}$, a Kriging model is expressed as follows [15]:

$$Y \approx \mathscr{M}^K(\boldsymbol{x}) = \boldsymbol{\gamma}^T\boldsymbol{F}(\boldsymbol{x}) + D(\boldsymbol{x}) \tag{10}$$

where $\boldsymbol{\gamma}^T\boldsymbol{F}(\boldsymbol{x})$ is the trend of the Kriging model, among them, $\boldsymbol{\gamma}$ represents the corresponding regression coefficient vector, $\boldsymbol{F}(\boldsymbol{x}) = [F_1(\boldsymbol{x}), \ldots, F_M(\boldsymbol{x})]$ is the polynomial basis function.

In addition, $D(\boldsymbol{x})$ is a Gaussian process with zero mean and covariance function defined as:

$$Cov\left(D(\boldsymbol{x}_i), D(\boldsymbol{x}_j)\right) = \sigma^2\Gamma\left(\boldsymbol{x}_i, \boldsymbol{x}_j; \boldsymbol{\Theta}\right) \tag{11}$$

where $\sigma^2$is the (constant) variance of $D(\boldsymbol{x})$, and $\Gamma(\boldsymbol{x_i}, \boldsymbol{x_j}; \boldsymbol{\Theta})$ is the correlation function, which describes the "similarity" between observation points,$D(\boldsymbol{x_i})$, and new points,$D(\boldsymbol{x_j})$, $\boldsymbol{\Theta} = [\boldsymbol{\Theta}_1, \ldots, \boldsymbol{\Theta_n}]^T$ is the hyperparameters of the correlation function.

Assuming that $\mathscr{Y} = \{\mathscr{M}(x^{(1)}), \ldots, \mathscr{M}(x^{(N)})\}$ obeys a multivariate Gaussian distribution, maximizing the likelihood function to estimate the unknown Kriging parameters $\boldsymbol{\delta} = (\boldsymbol{\gamma}, \sigma^2, \boldsymbol{\Theta})$ is as follows:

$$\mathscr{L}(\boldsymbol{\delta}; \mathscr{Y}) = \frac{(\det\boldsymbol{C})^{-1/2}}{(2\pi)^{N/2}}\exp\left[-\frac{1}{2}(\mathscr{Y} - \boldsymbol{G\gamma})^T C^{-1}(\mathscr{Y} - \boldsymbol{G\gamma})\right] \tag{12}$$

where the covariance matrix $\boldsymbol{C} = \sigma^2\boldsymbol{\Gamma} + \Sigma_n$, and among Σ_n is the noisy responses. $\boldsymbol{G} = [G(x_1), \ldots G(x_N)]^T$ is the $N \times M$ regression matrix with element$G_{ij} = G_j(x_i)$.

Taking the partial derivative of Eq. (12) with respect to $\boldsymbol{\gamma}$ and σ^2 to zeros, it can be translated into solving the following optimization problem to solve for the hyperparameters $\boldsymbol{\Theta}$ [33]:

$$\hat{\boldsymbol{\Theta}} = \underset{\boldsymbol{\Theta}\in\mathscr{D}_{\boldsymbol{\Theta}}}{argmin}[-\log\mathscr{L}(\boldsymbol{\Theta}; \mathscr{Y})] \tag{13}$$

Finally, the optimization problem in Eq. (13) is solved based on Covariance Matrix Adaptation–Evolution Strategy (CMA-ES) [34], then, the optimization problem can be written as:

$$\hat{\boldsymbol{\Theta}} = \underset{\boldsymbol{\Theta}\in\mathscr{D}_{\boldsymbol{\Theta}}}{argmin}\frac{1}{2}[\log(\det\boldsymbol{\Gamma}) + N\log\left(2\pi\sigma^2\right) + N] \tag{14}$$

2.1.4. Support vector regression

Support Vector Regression (SVR) was first developed in the 1990s [35]. Its core concept is that the original data is projected into a

high-dimensional feature space by using a kernel function, and then the best predictive function is found in the linear feature space. Roy [16] presented an in-depth introduction of SVR as a metamodeling tool for uncertainty quantification.

Supposed some input variables $\boldsymbol{x} \in \mathscr{D}_X \subset \mathbb{R}^M$ and the model outputs $Y = \mathscr{M}(\boldsymbol{x}) \in \mathbb{R}$, a linear SVR model is formulated as:

$$Y \approx \mathscr{M}^{SVR}(\boldsymbol{x}) = \boldsymbol{\varpi}^T \boldsymbol{x} + a \tag{15}$$

where $\boldsymbol{\varpi} = \sum_{i=1}^{N} (\Lambda_i - \Lambda_i^*)\boldsymbol{x}_i \in \mathbb{R}^n$ is a set of weight coefficient, Λ_i and Λ_i^* are positive Lagrange multipliers, and $a \in \mathbb{R}$ is an offset parameter to be estimated.

For nonlinear problems, by the nonlinear transform $\boldsymbol{x} \rightarrow \psi(\boldsymbol{x})$, the input variables can be mapped into a high or infinite dimensional feature space, thus, Eq. (15) can be extended as follows:

$$\mathscr{M}^{SVR}(\boldsymbol{x}) = \boldsymbol{\varpi}^T \psi(\boldsymbol{x}) + a = \sum_{i=1}^{N} (\Lambda_i - \Lambda_i^*) \psi(\boldsymbol{x}_i)^T \psi(\boldsymbol{x}) + a \tag{16}$$

where the inner product $\psi(\boldsymbol{x}_i)^T \psi(\boldsymbol{x})$ can be expressed as $k(\boldsymbol{x}_i, \boldsymbol{x})$, which is the so-called kernel function. In this study, the most popular Gaussian kernel, $k(\boldsymbol{x}_i, \boldsymbol{x}) = \exp\left(-\frac{\boldsymbol{x}_i - \boldsymbol{x}^2}{2\sigma^2}\right)$, is selected as the kernel function.

In addition, the Lagrange multipliers $\sigma_i$and σ_i^* can be solved by maximizing the Lagrangian function:

$$\begin{aligned} L(\Lambda, \Lambda^*) = & -\frac{1}{2} \sum_{i=1}^{N} \sum_{j=1}^{N} (\Lambda_i - \Lambda_i^*)\left(\Lambda_j - \Lambda_j^*\right) k(\boldsymbol{x}_i, \boldsymbol{x}_j) - \sum_{i=1}^{N} (\Lambda_i + \Lambda_i^*)\varepsilon \\ & + \sum_{i=1}^{N} (\Lambda_i - \Lambda_i^*) y_i, s.t. \ \sum_{i=1}^{N} (\Lambda_i - \Lambda_i^*) \\ & = 0 \text{ and } 0 \le \Lambda_i, \Lambda_i^* \le C, \ i = \{1, ..., N\}. \end{aligned} \tag{17}$$

where $C \in \mathbb{R}^+$ is a regularization parameter for the regression problem, ε is the insensitive tube width, which is the sparsity property to the SVR.

Next, the SVR model is then constructed by solving for the hyperparameters $\gamma = \{C, \varepsilon, \sigma\}^T$, and as same as in Kriging models, CMA-ES is used to find the optimal value of the hyperparameters.

2.2. Hybrid Particle Sswarm Optimization and Genetic Algorithm (HPSOGA)

GA is an approach to the search for optimal solutions by simulating the natural evolutionary process, inspired by the evolution of organisms in nature [36]. The algorithm converts the problem solution into a process resembling the crossover and mutation of chromosomal genes, where the fitness of each chromosome is evaluated based on an objective function. This process usually continues for several generations to obtain a best-fit (near-optimal) solution, ensuring the quality of the offspring population is always better than that of the parents [37]. There are various types of GA applied to engineering problems, in which real-coded GAs have become the most popular for their simplicity and effectiveness [38,39].

PSO is a stochastic optimization algorithm developed by Eberhart and Kennedy [40], which is inspired by the social behaviors of swarming organisms, such as the foraging behavior of a flock of birds. The basic idea is to exploit the sharing of information among individuals, so that the movement of the whole population evolves from disorder to order in the problem solution space, and thus obtain an optimal solution to the problem [41].

It is commonly acknowledged that with global search capacity, PSO is an effective algorithm to deal with optimization problems. Nevertheless, since PSO relies heavily on the quality of the initial population, and if the position of the initial population is far from the global best, it may be difficult to find the optimal solution [42]. To compensate for this drawback of PSO, this study adopts a hybrid PSO and GA (HPSOGA). First, the crossover and mutation capacity of GA is used to generate initial high-quality populations, after that the global search capacity will be employed to look for the optimal solutions. The working principle of the HPSOGA (see Fig. 2) are depicted as follows [43,44]:

Step 1: Initialize each variable of GA.
Step 2: Calculate the local best populations and rank them in increasing order depending on the objective function.
Step 3: Introduce the best populations as the parents for crossover and mutation in GA.
Step 4: Choose the best offspring populations after crossover and mutation for the next iteration.
Step 5: Repeat steps 3 to 4 until the best population in GA meets the termination criteria, i.e. the number ofiterations =100.
Step 6: Based on the global search capability of PSO, the populations obtained from step 5 are used to find the best solution. More specific steps are: (i) updated velocity and position of particles in PSO and (ii) select the local best for the current iteration and the global best for the next iteration based on the greedy strategy.
Step 7: Repeat step 6 until termination criteria is satisfied.
Step 8: The iterations process is completed with the best solution.

3. Proposed parameter identification method: MA-HPSOGA

The procedure of the proposed MA-HPSOGA method to identify structural unknown parameters is described in detail below.

Step 1: Building computational model and selecting input parameters: The first step in the work is to build a high-precision FE model that adequately reflects the structural properties, followed by setting the input parameters. Usually, due to some uncertainty exists in the modeling and measurement, it is difficult to obtain the exact values of these input parameters. Therefore, we need to select some unknown input parameters that have a significant impact on the structural response.
Step 2: Preparing the initial dataset for metamodeling: The uncertainty of the unknown input parameters is usually expressed in the form of a probabilistic model. Hence, the probabilistic model (known distribution type, mean, deviation) is first given, and then the input dataset is generated using the Latin High Cube Sampling (LHS) method. Next, a probabilistic FEA is performed to extract the corresponding structural system response (or Quantity of Interests - QoIs) as the output dataset. Finally, the "input-output" dataset is integrated to form the initial dataset for constructing the metamodel.
Step 3: Constructing and evaluating metamodels: The initial dataset will be divided into two parts. In the first part, Design of experiments (DoE) [45] will be used to construct the selected four metamodels (PCE, Kriging, SVR, ANN), and in the second part, a validate dataset will be used to verify their predictive accuracy.
Step 4: Constructing the objective function: Selecting high precision metamodels to substitute time-consuming FE models for predicting structural system response, and then integrating into the objective function together with the measured structural system response.
Step 5: Optimizing the objective function: The HPSOGA is adopted to optimize the objective function, and after the evolution curve of the fitness reaches convergence, the optimal population position is output as the identification value of the unknown input parameters.
Step 6: Model updating: Updating the finite element model with parameter identification and comparing the structural system response before and after model updating.

A detailed description of the MA-HPSOGA method for model updating is presented in Fig. 3.

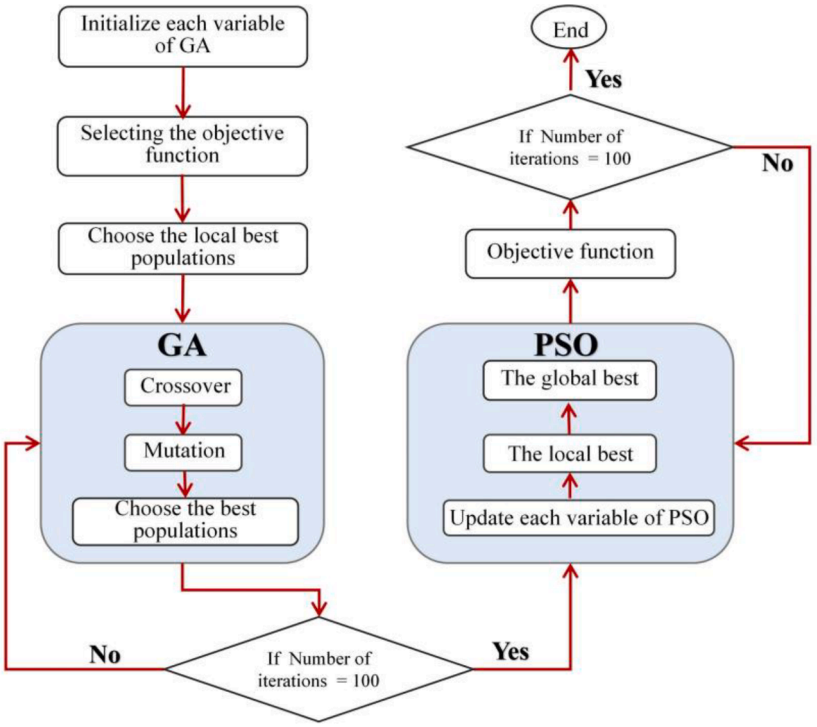

Fig. 2. The working principle of HPSOGA.

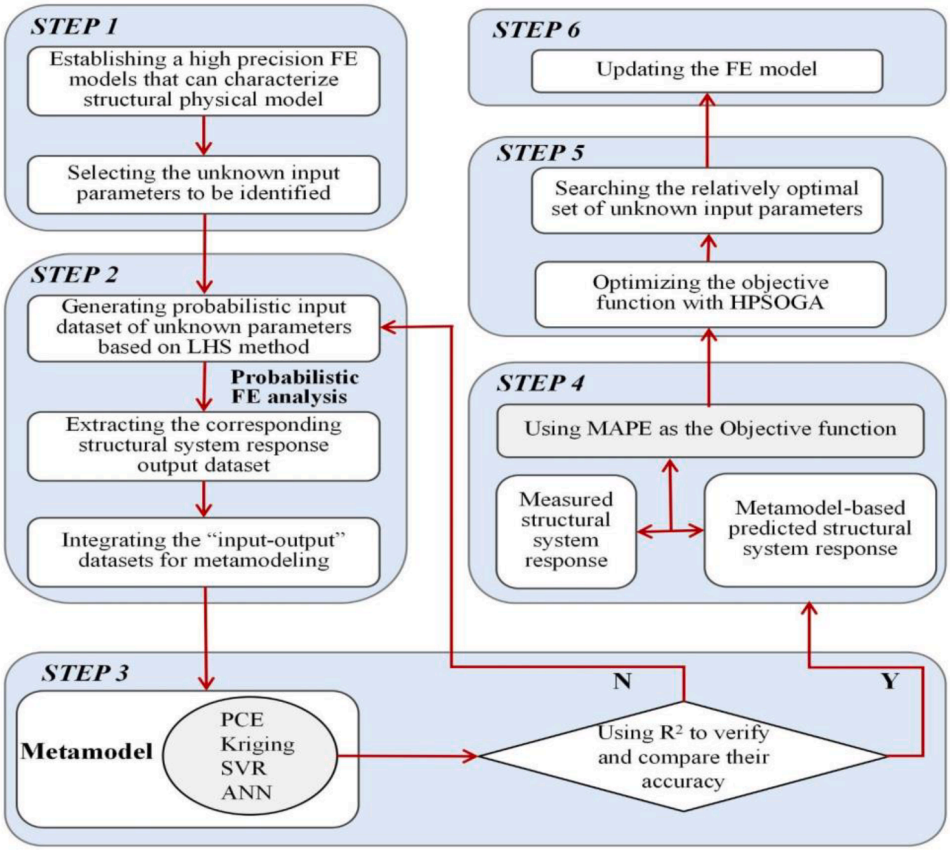

Fig. 3. Flowchart to describe MA-HPSOGA for model updating.

3.1. Metrics to evaluate MA-HPSOGA

First, R-squared (R^2) [46] is adopted to verify the predictive accuracy of the above four metamodels, and it is formulated as shown below:

$$R^2 = 1 - \frac{\sum_{i=1}^{n}\left(y_{val,i} - y_{pre,i}\right)^2}{\sum_{i=1}^{n}\left(y_{val,i} - \bar{y}_{val}\right)^2} \in [0,1] \tag{18}$$

where $y_{val,i}$ is the output value of the structural response in the validation dataset,$y_{pre,i}$ is the predicted value of the metamodel corresponding to $y_{val,i}$ and $\bar{y}_{val}$ is the mean of the output value in the validation dataset.

In addition, the Mean Absolute Percentage Error (MAPE) [46] is used to evaluate the accuracy of the MA-HPSOGA method due to its intuitive percentage representation, which is expressed as follows:

$$MAPE = \frac{100\%}{n}\sum_{i=1}^{n}\frac{\left|y_{M,i} - y_{P,i}\right|}{y_{M,i}} \tag{19}$$

where $y_{M,i}$ is the measured value of the structure output response, $y_{P,i}$ is the predicted value based on metamodel, and n is the number of fitted points.

4. Validation of MA-HPSOGA

This section validates the effectiveness of the MA-HPSOGA method for model updating by studying a cantilever aluminum plate.

4.1. Model and experimental setup

An AL6061-T6 aluminum alloy plate, with dimensions of 600 × 400 × 3 mm^3, is anchored in the fixture at a depth of 100 mm embedded, thus leading to a cantilevered plate of 500 × 400 × 3 mm^3, see Fig. 4(a). The plate has a calibrated elastic modulus of 710 MPa and a density of 2700 kg/m^3.

To accurately acquire the natural frequencies of the cantilevered aluminum plate, two popular Experimental Modal Analysis (EMA) methods are used: the hammering method and the sweep frequency method and the experimental setup to perform EMA for the cantilever plate as shown in Fig. 4(a). A Piezoelectric Lead-Zirconate–Titanate (PZT) actuator is surface-bonded to the bottom center on the back of the cantilever plate for receiving the excitation signal, which was generated by an Agilent® 33250A wave signal generator, with a sweep sine excitation ranging from 100 to 2000 Hz, and then amplified by a Pintek® HA-405 high voltage amplifier with a voltage amplitude of 200 Vpp [47]. The vibration response of the plate was measured by a Polytec® PSV-400 Scanning Laser Doppler Vibrometer (SLDV), and the Frequency Response Functions (FRFs) are obtained based on the FFT method. According to Fig. 4(b), the peak amplitude locations identified by the two methods are in high consistency, and the first ten peak frequencies were extracted as the measured QoIs.

4.2. Construction of parameter prior distribution space

Assuming that the elastic modulus and density of the aluminum plate are unknown input parameters and obey lognormal distribution, their experimental calibration values are the distribution mean. With a 10% standard deviation, and then the LHS method is used for sampling to construct the prior distribution space of the input parameters, as shown in Table 1. The finite element model of the cantilever plate is built using shell elements, with dimensions of 25×20×1 mm^3, and then, a subset of the computed natural frequencies of the aluminum plate is extracted by probabilistic FEA as the calculated QoIs.

4.3. Results and discussions

In this section, the construction of the metamodel and the MA-HPSOGA method for identifying the unknown parameters of the cantilevered aluminum plate are described in detail.

The unknown input parameters E and ρ were randomly sampled 35 times by the LHS method, and then the probabilistic FEA (modal analysis) was performed to extract ten calculated natural frequency subsets, which correspond to the measured QoIs. Based on this, the initial 35 sets of "input-output" datasets were generated.

There is no solid recommendation for the sampling size of DoE, however, there are some suggestions that might be problem-dependent: (a) $\frac{N\times(N+1)}{2}$ and (b) $10\times N$, where N is the number of input parameters [48,49]. From these suggestions, we can observe that the size of DoE is positively correlated with N. In addition, to explore the modeling capabilities of these four metamodels with small sample sets, a trade-off is made in choosing the size of the DoE. Considering two input parameters in this case, the first 15 sets as DoE are used to construct these four metamodels, and the last 20 sets as validate dataset are used to verify the predictive accuracy of these metamodels. Next, these developed metamodels with reliable accuracy are coupled with HPSOGA respectively. The following notations specify each combination: PCE_HPSOGA, Kriging_HPSOGA, SVR_HPSOGA, ANN_HPSOGA.

In this study, all numerical computing environments are based on a

Table 1
Material properties for the cantilever aluminum plate.

Unknown Parameters	Unit	Symbol	Model	Quantity
Density	kg/m^3	ρ	Lognormal	*LN* (710, 71)
Elastic Modulus	MPa	*E*	Lognormal	*LN* (2700, 270)
Poisson's ratio	–	*ν*	Constant	0.3

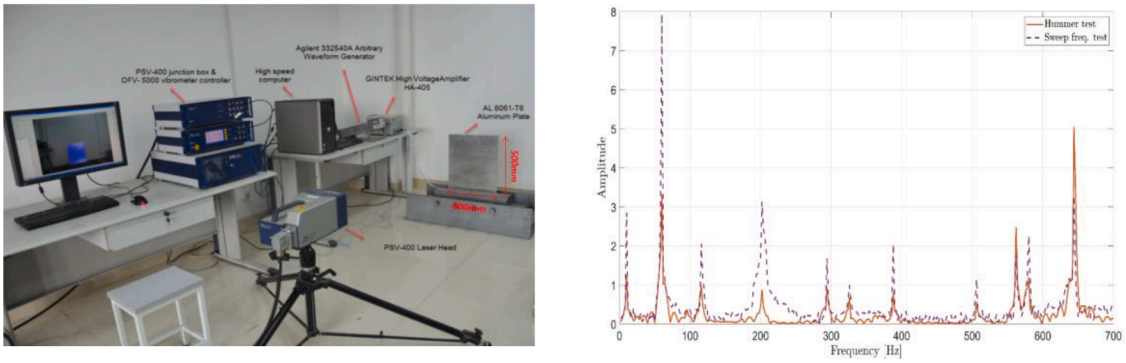

Fig. 4. Experimental setup and results for a modal analysis of a cantilever aluminum plate: (a) required experimental devices adopted from [47] and (b) Frequency Response Function based on hammer test and sweep frequency test. (For interpretation of the references to colour in this figure legend, the reader is referred to the web version of this article.)

high-performance UNIX workstation, which has two nodes, each node has a 36-core CPU and 192 GB of memory. The probabilistic FEA is executed in ANSYS APDL [50] by calling a 12-core CPU, in addition, the PCE, Kriging and SVR models are constructed based on the open-source software UQLab [51]. The ANN model is based on BPNN, and then, the combination of these metamodels with HPSOGA is also implemented in MATLAB. In order to keep fairness, the basic parameters in HPSOGA are the same in this study.

Hereafter, four methods are used to identify the structural unknown input parameters, and the results are shown in Table 2. Furthermore, some results are shown in Fig. 5 and Table A.5 with the following major observations:

- Regarding the predictive accuracy of the metamodels, we can see from Fig. 5(a) that the PCE and Kriging models basically achieve a near perfect prediction (R^2 is close to 1), and the SVR and ANN models also have high predictive accuracy, with their R^2 being greater than 0.98. Thus, all four metamodels can reliably substitute the cantilevered aluminum plate.
- The total computation time of the MA-HPSOGA method is divided into two parts: part 1 is the time consumed to construct these metamodels, which is the same since the same initial dataset is used, and the part 2 is the running time of the MA-HPSOGA method in MATLAB. From Fig. 5(a), we can intuitively observe that the PCE_HPSOGA method has the highest computational efficiency, and next is ANN_HPSOGA. Kriging_HPSOGA has the lowest computational efficiency, although the Kriging model has a perfect predictive accuracy. This is because there is no hyperparameter optimization process involved in the PCE model, however, the other three models have to optimize hyperparameters to improve the predictive accuracy of the model.
- We can observe that the accuracy of the four methods is very close (see Table A.5), the highest accuracy is for SVR_HPSOGA (MAPE is 0.8374%), and the lowest accuracy is for ANN_HPSOGA (MAPE is 0.8912%). This can be used to demonstrate the effectiveness of the MA-HPSOGA method for model updating, since here the material parameters of the aluminum plate have an exact calibration value.
- From Fig. 5(b), there are slight differences in the convergence speed and robustness of the four methods, and it is easy to observe that the PCE_HPSOGA method has the best performance in these two aspects. In addition, the SVR_HPSOGA method, despite its better performance in escaping the local optimum, has a convergence speed that is far from that of the other three methods.

Based on the above analysis, the PCE_HPSOGA method stands out among the four methods. For a more intuitive observation, the parameters obtained by the PCE_HPSOGA method were used for the FE model updating, and the results are shown in Fig. 6. As it can be clearly seen, the frequency curves constructed from the first 150 orders of calculated natural frequencies almost overlap before and after the model updating. Moreover, the ten measured frequency points are almost distributed on both curves, which directly provides convincing evidence for the effectiveness of the MA-HPSOGA method.

5. Application of MA-HPSOGA to small-scaled dam

The previous section provides a detailed validation for the effectiveness of the MA-HPSOGA method applied to model updating. This section will take a small-scaled laboratory model as example, to further explore the applicability of the MA-HPSOGA method to practical engineering problems.

5.1. Model and experimental setup

The small-scaled dam was built as a prototype of the WuDongde Arch Dam, a super-high hyperbolic arch dam, with a height of 270 m. By truncating the boundaries around the prototype dam and at a scale of 1:200, a small-scaled laboratory dam model is constructed as shown in Fig. 7(a). The laboratory dam consists of two parts: the dam and the foundation, where the foundation is made of C30 concrete. However, the material of the dam is modulated according to the principle of material ratio in the scale experiment [52]. In addition, an isosceles FE model is built using the hexahedral and tetrahedral isoperimetric elements, and the detailed dimensional drawings are shown in Fig. 7(b).

Fig. 8(a) shows the required experimental devices for the EMA of the small-scaled laboratory model. Eight 1A202E® low-frequency piezoelectric accelerometers are installed on the dam, seven of which are equally positioned at the crest of the dam and one at the upstream dam face. The vibration response of the model is excited by hammer tests, and the time-domain signal of the system response is collected by the DH5972N® online monitoring and analysis system. Finally, the FRF of the small-scaled dam is obtained based on the FFT method, as shown in Fig. 8(b), and the first eight peak frequencies as the measured QoIs are tabulated in Table A.6.

5.2. Construction of parameter prior distribution space

It is assumed that the elastic modulus and density of the dam and foundation are unknown input parameters, and both obey normal distribution, where the measured average value of the sampled specimens in the dam material is taken as the mean of its distribution function, and the normative value of C30 concrete is used as that for the foundation. Considering the uncertainty of modeling and measurement, a standard deviation of 10% is given, and these material properties are listed in Table 3. A subset of the calculated natural frequencies of the small-scale dam, corresponding to the measured QoIs, was extracted as the calculated QoIs, and all numerical environments are the same as in Section 4.

5.3. Comparison and remarks

In this section, the MA-HPSOGA method is applied to the small-scaled laboratory dam model with significant measurement and material uncertainty.

The same procedure as in Section 4.3 is performed to generate the initial 50 sets of "input-output" datasets, of which the first 20 sets as DoE were used to construct these metamodels, and the last 30 as validate dataset were used to verify their predictive accuracy. The predictive accuracy of the four metamodels is evaluated by the R^2 metric, and then, they are combined with HPSOGA. Furthermore, to highlight the superiority of the coupled approach, the HPSOGA combined with the FE model directly is used to optimize the unknown input parameters. This process is based on a co-simulation with MATLAB and ANSYS APDL, and the similar notations specify their combination: FEM_HPSOGA.

The results of parameter identification based on above five methods are shown in Table 4, besides, Table A.6 and Fig. 9 further illustrate the computational accuracy and efficiency of these method. Some observations are as follows:

Table 2
Parameter identification results for cantilever aluminum plate.

Parameters	Unit	PCE_HPSOGA	Kriging_HPSOGA	SVR_HPSOGA	ANN_HPSOGA
ρ	kg/m^3	2726.748	2545.189	2431.344	2719.301
E	MPa	708.834	661.383	638.685	703.077

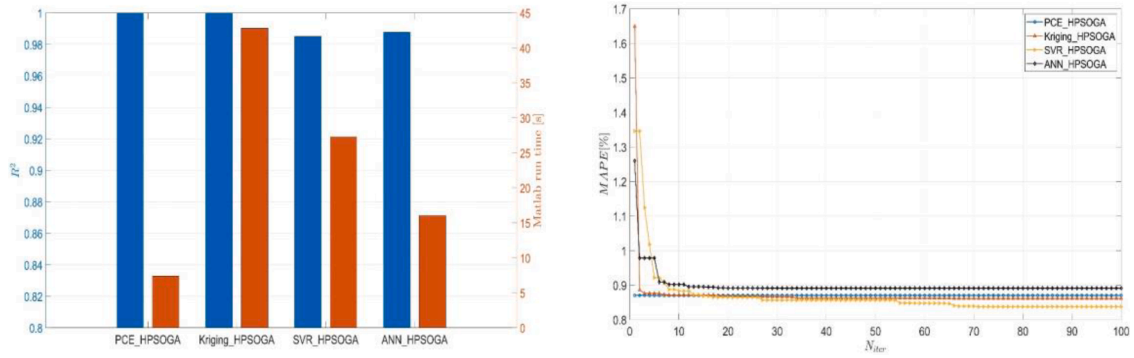

Fig. 5. Construction of metamodel and MA-HPSOGA method for cantilever aluminum plate: (a) the predictive accuracy of metamodels and calculation time of the MA-HPSOGA method and (b) the accuracy of the MA-HPSOGA method. (For interpretation of the references to colour in this figure legend, the reader is referred to the web version of this article.)

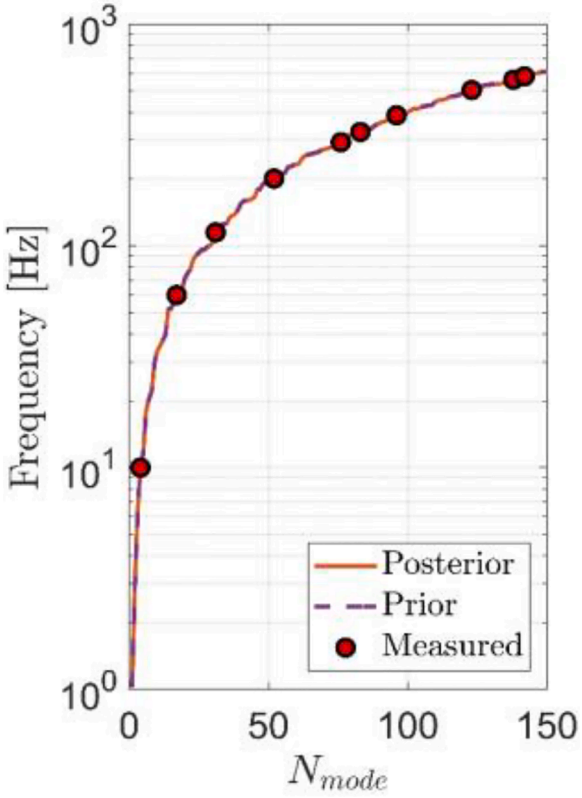

Fig. 6. Comparison of results before and after model updating based on PCE_HPSOGA.

- From Fig. 9(a), we can intuitively find that the predictive accuracy of the SVR model (R^2=0.8659) is significantly lower than that of the other three metamodels (R^2 >0.98), which is far from the prediction in the cantilevered plate in Fig. 5(a), indicating that the SVR model is not as applicable as the other three metamodels in complex structures.
- Comparing Fig. 5(a) and Fig. 9(a), we can make some interesting observations: the PCE_HPSOGA method always has the shortest running time in MATLAB, while the Kriging_HPSOGA method always has the longest, and the other two methods have moderate performance. This further demonstrates the excellent performance and theoretical superiority of the PCE model, bypassing the hyperparametric optimization process while still producing high-quality predictions. However, the other three metamodels, subject to hyperparameter optimization, always have difficulty in balancing predictive accuracy and computational efficiency.

- Comparing the computational accuracy of the MA-HPSOGA method for parameter identification, we can easily observe from Fig. 5(b) and Fig. 9(b) that there are significant differences in the evolutionary curves of the fitness values between the two. This is because the input parameters in the simple cantilever plate have precisely calibrated values (with little material uncertainty), so that all four evolutionary curves in Fig. 5(b) almost converge to the global optimum. However, when the complexity (more unknown parameters, more complicated FE models, etc.) and uncertainties (materials, measurements, etc.) of the applied object increase, the differences in performance between the four MA-HPSOGA methods come to the fore.
- Furthermore, to illustrate the superiority of the MA-HPSOGA method, a conventional parameter identification method that directly combines the HPSOGA algorithm with the structural FE model for iterative optimization is adopted for comparison. As it can be seen from Fig. 9(b) and Table A.6, the FEM_HPSOGA method has difficulty in reconciling computational accuracy and efficiency. Although the method has a moderate computational accuracy among the five methods, its computational cost (approximated to 83.354 h) is 24.85 times higher than the other four MA-HPSOGA methods (approximated to 3.355 h).
- Notably, ANN models are not usually prone to highly reliable prediction accuracy in small sample sets. However, they consistently perform well in both cases, and the following two reasons may explain this situation.

(1) Dataset is well structured: the strong mapping relationship between input (material parameters) and output (natural frequencies), therefore, the ANN models still work effectively with small samples.
(2) In both cases, the input parameters are few, reducing the possibility of high-dimensional nonlinear mappings.

Overall, it is gratifying to note that the PCE_HPSOGA method not only has the highest computational efficiency, but also has the obvious highest computational accuracy. Hence, the PCE model is used as a pilot model and combined with two popular sub-algorithms in HPSOGA: PSO and GA. The following notation specifies each combination: PCE_PSO and PCE_GA. The results are shown in Fig. 10(a), from which we can draw some conclusions as follows:

- Compared to the PCE_PSO method, the PCE_HPSOGA method converges significantly faster, although their final convergence accuracy is almost the same. The PCE_PSO method requires nearly 50 iterations to reach convergence of the evolutionary curves of the fitness

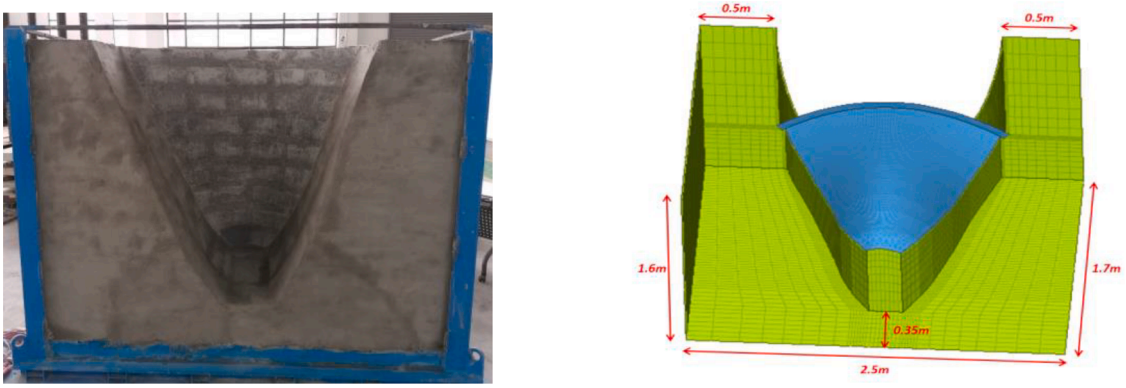

Fig. 7. Physical and numerical model of a small-scaled dam model: (a) laboratory model and (b) FE model.

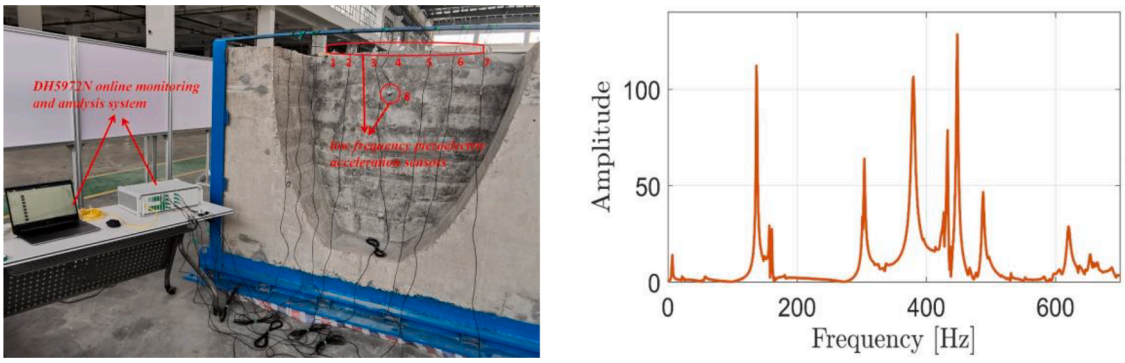

Fig. 8. Experimental setup and results for modal analysis of a small-scaled dam model: (a) experimental devices and (b) Frequency Response Function based on hammer test.

Table 3
Material properties for the small-scaled experimental arch dam.

Component Name	Unknown Parameters	Unit	Symbol	Model	Quantity
1-Dam	Density	kg/m^3	ρ_1	Normal	N (1.5, 0.15)
	Elastic Modulus	GPa	E_1	Normal	N (2200, 220)
	Poisson's ratio	–	ν_1	Constant	0.22
2-Foundation	Density	kg/m^3	ρ_2	Normal	N (30, 3)
	Elastic Modulus	GPa	E_2	Normal	N (2400, 240)
	Poisson's ratio	–	ν_2	Constant	0.19

values, while the PCE_HPSOGA method converges in less than 30 iterations, resulting from the fact that the GA provides a better initial search space for the HPSOGA and thus improves its convergence speed.

- Compared with the PCE_GA method, the PCE_HPSOGA method not only has a faster convergence rate, but also has higher accuracy and stronger robustness, attributed to the fact that PSO searches the optimal solution by updating the position and velocity between particles, thus allowing the HPSOGA to have better performance.

For more intuitive view on the effectiveness of the MA-HPSOGA method for FE model updating, the parameter identification values obtained by the best-performing PCE-HPSOGA method are used to update the FE model, and the results are shown in Fig. 10(b). As it can be clearly seen, the frequency curves constructed from the first 30 orders of calculated natural frequencies are clearly separated before and after the model updating, which differs significantly from those in Fig. 6. Moreover, it is clear that the eight measured frequency points are distributed more closely to the posterior frequency curve after the model updating.

6. Conclusions

In the real world, almost all complex structures, such as bridges and dams, are fraught with numerous uncertainties. Their values of material parameters are often difficult to measure accurately due to the complex construction environment and processes, as well as the extremely long construction periods. Therefore, identifying the most accurate material parameters, making the response of the structural FE model as close as possible to the real structural system response, becomes a priority in structural safety assessment.

Table 4
Parameter identification results for small-scaled dam.

Parameters	Unit	PCE_HPSOGA	Kriging_HPSOGA	SVR_HPSOGA	ANN_HPSOGA	FEM_HPSOGA
ρ_1	kg/m^3	2660.042	2838.398	2453.388	1937.711	2426.167
E_1	GPa	1.622	1.655	1.441	1.170	1.485
ρ_2	kg/m^3	2587.024	2531.169	2663.781	2072.919	2740.946
E_2	GPa	32.694	38.305	27.338	34.346	23.806

Table A.5
Comparison of measured and predicted natural frequencies for cantilever aluminum plate.

Modes	Measured frequency [Hz]	PCE_HPSOGA	Kriging_HPSOGA	SVR_HPSOGA	ANN_HPSOGA
1	10	10.30	10.31	10.33	10.30
2	60	58.55	58.58	58.71	58.69
3	115	113.94	113.97	114.02	113.87
4	201	201.15	201.03	201.40	201.01
5	293	289.38	289.48	290.13	289.03
6	326	326.00	326.00	326.28	326.35
7	388	386.93	386.92	387.61	387.13
8	504	503.43	503.55	504.00	503.89
9	561	561.74	561.89	561.00	563.08
10	581	583.98	584.29	585.11	584.63
R^2		0.9999	0.9999	0.9851	0.9877
MAPE		0.870%	0.863%	0.837%	0.905%
Runtime in MATLAB [Sec]		7.397	42.817	25.442	16.025

Table A.6
Comparison of measured and predicted natural frequencies for small-scaled dam.

Modes	Measured frequency [Hz]	PCE_HPSOGA	Kriging_HPSOGA	SVR_HPSOGA	ANN_HPSOGA	FEM_HPSOGA
1	137	139.33	140.45	137.67	139.72	139.35
2	157	143.01	144.35	141.24	144.67	140.89
3	304	313.52	316.29	310.81	313.07	315.64
4	379	375.69	377.19	371.80	377.83	377.12
5	433	433.01	431.40	421.72	428.55	425.29
6	448	448.00	441.65	452.61	456.96	452.77
7	480	488.00	488.07	496.23	488.00	492.36
8	620	619.96	621.49	620.00	620.02	621.42
R^2		0.985	0.989	0.866	0.996	–
MAPE		1.8374%	2.1684%	2.4997%	2.0207%	2.347%
Part 1 [Sec]		12.163	60.686	34.209	27.512	–
Part 2 [hr]		3.35	3.35	3.35	3.35	–
Total time[hr]		3.352	3.361	3.356	3.355	83.354

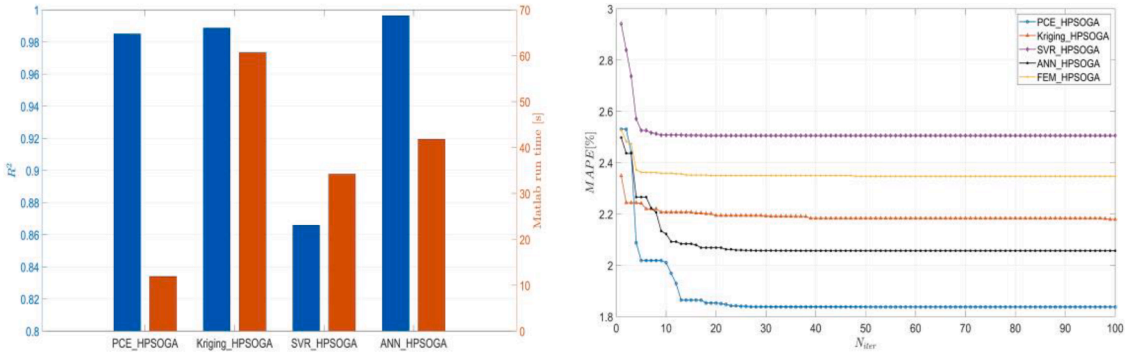

Fig. 9. Comparison of the computational efficiency and accuracy of five methods: (a) the predictive accuracy of metamodels and computational efficiency of the MA-HPSOGA method and (b) the computational accuracy of five methods. (For interpretation of the references to colour in this figure legend, the reader is referred to the web version of this article.)

In this study, the unknown material parameters are first randomly sampled based on the LHS method under a specified probability distribution model. Then a probabilistic FEA is performed to extract the initial "input-output" dataset for constructing these metamodels. Further, four popular metamodels (PCE, Kriging, SVR, ANN) are constructed based on this dataset, and their accuracy is evaluated by the commonly used validation metric R^2. Next, the objective function is constructed based on the measured and predicted natural frequencies based on these metamodel, which is optimized using HPSOGA. Finally, the presented MA-HPSOGA method is used to identify the unknown input parameters of the structure. Some conclusions were summarized as follows:

- The PCE, Kriging, and ANN models have high predictive accuracy for both simple cantilevered plate and complex laboratory dam, while the SVR model is dwarfed by the predictive capability in complex structures.
- From four perspectives: computational accuracy and efficiency, convergence speed and robustness, the practicality of the MA-HPSOGA method in complex structure is judged. Undoubtedly, the PCE_HPSOGA method comes out on top in terms of the overall performance. SVR_HPSOGA method is not considered a suitable choice under the optional prerequisite, considering the relatively poor predictive ability of the SVR model.
- In comparison with the traditional FEM_HPSOGA method, the MA-HPSOGA method shows unparalleled superiority. With the selection of a suitable metamodel, not only can the computational efficiency be greatly improved, but even the computational accuracy can be moderately improved.

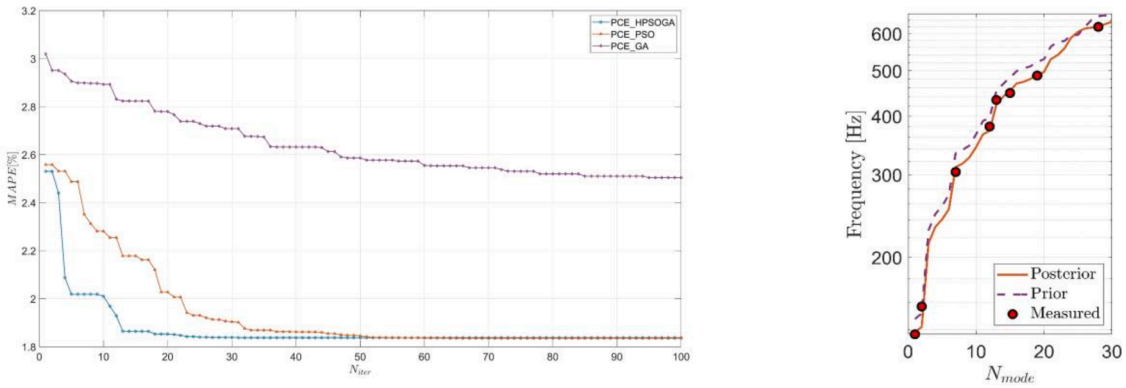

Fig. 10. Some visual results based on the PCE_HPSOGA method: (a) comparison of the accuracy between PCE_HPSOGA method and other two methods and (b) comparison of results before and after FE model updating based on PCE_HPSOGA.

In summary, the PCE_HPSOGA method has an excellent ability to identify the structural unknown parameters, which can provide sufficient guarantees for building high-fidelity FE models, and the target structure can be extended to any large and complex structures. However, there are still some shortcomings that need to be pointed out in this type of method.

- The precision of the surrogate model is subject to the classical "curse of dimensionality", which makes it difficult to build reliable surrogate models for high-dimensional problems. This approach is difficult to apply in this situation.
- Generating an initial dataset for constructing the metamodel accounts for nearly all the overall computational expenses of this approach to solving the model update problem. If the initial computational models demand substantial computational resources, for example, simulation of complex systems that require a single simulation measured in days, the entire efficiency of this approach will be significantly reduced.
- The type of probabilistic distribution that the material parameters obey is based on a priori knowledge and may deviate somewhat from the real world. It is reasonable to infer the type in advanced based on specimen sampling tests.

In the future, we will further extend the application of this approach in damage identification for complex and nonlinear structural.

CRediT authorship contribution statement

Li YiFei: Investigation, Methodology, Validation, Writing – original draft. **Cao MaoSen:** Investigation, Methodology, Validation, Supervision, Writing – review & editing. **Tran N. Hoa:** Software, Investigation. **S. Khatir:** Software, Investigation. **Hoang-Le Minh:** Software, Investigation. **Thanh SangTo:** Software, Investigation. **Thanh Cuong-Le:** Validation, Writing – review & editing. **Magd Abdel Wahab:** Investigation, Methodology, Validation, Supervision, Writing – review & editing.

Declaration of Competing Interest

The authors declare that they have no known competing financial interests or personal relationships that could have appeared to influence the work reported in this paper.

The authors declare the following financial interests/personal relationships which may be considered as potential competing interests:

Data availability

The data that has been used is confidential.

Acknowledgement

The authors are grateful for the Fundamental Research Funds for the Central Universities: No.B220204002; the 2022 National Young Foreign Talents Program of China: No.QN2022143002L; the Jiangsu International Joint Research and Development Program (No. BZ2022010); the Nanjing International Joint Research and Development Program (No. 202112003).

Appendix A. Detailed Results

XXX

References

[1] Griebel M, Dornseifer T, Neunhoeffer T. Numerical simulation in fluid dynamics: a practical introduction. Society for Industrial and Applied Mathematics; 1998 [M].
[2] Sehgal S, Kumar H. Structural dynamic model updating techniques: a state of the art review. Arch Comput Meth Eng 2016;23(3):515–33.
[3] Ereiz S, Duvnjak I, Jiménez-Alonso JF. Review of finite element model updating methods for structural applications. Elsevier; 2022. p. 684–723 [C]//Structures41.
[4] Wang JT, Wang CJ, Zhao JP. Frequency response function-based model updating using Kriging model. Mech Syst Signal Process 2017;87:218–28.
[5] Mottershead JE, Link M, Friswell MI. The sensitivity method in finite element model updating: a tutorial. Mech Syst Signal Process 2011;25(7):2275–96.
[6] Bakir PG, Reynders E, De Roeck G. Sensitivity-based finite element model updating using constrained optimization with a trust region algorithm. J Sound Vib 2007; 305(1–2):211–25.
[7] Tran-Ngoc H, Khatir S, Le-Xuan T, et al. Finite element model updating of a multispan bridge with a hybrid metaheuristic search algorithm using experimental data from wireless triaxial sensors. Eng Comput 2021:1–19.
[8] Dinh-Cong D, Nguyen-Thoi T. An effective damage identification procedure using model updating technique and multi-objective optimization algorithm for structures made of functionally graded materials. Eng Comput 2021:1–19.
[9] Minh HL, Sang-To T, Wahab MA. Structural damage identification in thin-shell structures using a new technique combining finite element model updating and improved Cuckoo search algorithm. Adv Eng Software 2022;173:103206.
[10] Sang-To T, Hoang-Le M, Khatir S, et al. Forecasting of excavation problems for high-rise building in Vietnam using planet optimization algorithm. Sci Rep 2021; 11(1):1–10.
[11] Wu H, Wu P, Xu K, et al. Finite element model updating using crow search algorithm with Levy flight. Int J Numer Methods Eng 2020;121(13):2916–28.
[12] Li YF, Hariri-Ardebili MA, Deng TF. A surrogate-assisted stochastic optimization inversion algorithm: parameter identification of dams. Adv Eng Inf 2023;55: 101853.
[13] Wang C, Li Y, Tran NH. Artificial neural network combined with damage parameters to predict fretting fatigue crack initiation lifetime. Tribol Int 2022;175: 107854.
[14] YiFei L, MaoSen C, Tran-Ngoc H, et al. Multi-parameter identification of concrete dam using polynomial chaos expansion and slime mould algorithm. Comput Struct 2023;281:107018.
[15] Santner T, Williams B, Notz W. The design and analysis of computer experiments. Springer; 2003. Springer series in Statistics.
[16] Roy A, Chakraborty S. Support vector regression based metamodel by sequential adaptive sampling for reliability analysis of structures. Reliab Eng Syst Saf 2020; 200:106948.
[17] Zhou K, Tang J. Structural model updating using adaptive multi-response Gaussian process meta-modeling. Mech Syst Signal Process 2021;147:107121.

[18] Naranjo-Pérez J, Infantes M, Jiménez-Alonso JF, Sáez A. A collaborative machine learning-optimization algorithm to improve the finite element model updating of civil engineering structures. Eng Struct 2020;225:111327.
[19] Wang FY, Xu YL, Zhan S. Multi-scale model updating of a transmission tower structure using Kriging meta-method. Struc Control Heal Monitor 2017;24(8): e1952.
[20] Xia Z, Li A, Shi H, et al. Model updating of a bridge structure using vibration test data based on GMPSO and BPNN: case study. Earthquake Engin Engin vibration 2021;20(1):213–21.
[21] Tran-Ngoc H, Khatir S, Ho-Khac H, et al. Efficient Artificial neural networks based on a hybrid metaheuristic optimization algorithm for damage detection in laminated composite structures. Compos Struct, 262; 2021, 113339.
[22] Maind SB, Wankar P. Research study on basic of artificial neural network. Int J Recent Innov Trends Comp Commun 2014;2(1):96–100.
[23] Yilmaz I, Yuksek AG. An example of artificial neural network (ANN) application for indirect estimation of rock parameters. Rock Mech Rock Eng 2008;41(5):781.
[24] Ernst OG, Mugler A, Starkloff H-J, Ullmann E. On the convergence of generalized polynomial chaos expansions. ESAIM: Math Modell Numer Anal 2012;46:317–39.
[25] Soize C, Ghanem R. Physical systems with random uncertainties: chaos representations with arbitrary probability measure. SIAM J Sci Comput 2004;26: 395–410.
[26] Blatman G, Sudret B. Adaptive sparse polynomial chaos expansion based on least angle regression. J Comput Phys 2011;230:2345–67.
[27] Fajraoui N, Marelli S, Sudret B. Sequential design of experiment for sparse polynomial chaos expansions. SIAM/ASA J Uncert Quantific 2017;5:1061–85.
[28] Luthen N, Marelli S, Sudret B. Sparse polynomial chaos expansions: literature survey and benchmark. SIAM/ASA J Uncert Quantific 2021;9:593–649.
[29] YiFei L, Minh HL, Khatir S, et al. Structure damage identification in dams using sparse polynomial chaos expansion combined with hybrid K-means clustering optimizer and genetic algorithm. Eng Struct 2023;283:115891.
[30] Efron B, Hastie T, Johnstone I, Tibshirani R, et al. Least angle regression. Annals Statist 2004;32:407–99.
[31] Krige DG. A statistical approach to some mine valuation and allied problems on the witwatersrand. University of the Witwatersrand, South Africa; 1951. Master's thesis.
[32] Sacks J, Welch WJ, Mitchell TJ. Design and analysis of computer experiments. Statist Sci 1989;4(4):409–23.
[33] Dubourg V. Adaptive surrogate models for reliability analysis and reliability-based design optimization. Université Blaise Pascal-Clermont-Ferrand II; 2011 [D].
[34] Hansen N, Ostermeier A. Completely derandomized self-adaptation in evolution strategies. Evol Comput 2001;9(2):159–95.
[35] Vapnik V. The nature of statistical learning theory. Springer; 1995.
[36] Katok S, Chauhan SS, Kumar V. A review on genetic algorithm: past, present, and future. Multimed Tools Appl 2021;80(5):8091–126.
[37] Tran-Ngoc H, Khatir S, De Roeck G, et al. Model updating for Nam O bridge using particle swarm optimization algorithm and genetic algorithm. Sensors 2018;18 (12):4131.
[38] Mirjalili S. Genetic algorithm [M]//. Evolutionary algorithms and neural networks. Cham: Springer; 2019. p. 43–55.
[39] Katoch S, Chauhan SS, Kumar V. A review on genetic algorithm: past, present, and future. Multimed Tools Appl 2021;80(5):8091–126.
[40] Kennedy J, Eberhart R. Particle swarm optimization [C]//. In: Proceedings of ICNN'95-international conference on neural networks. IEEE; 1995. p. 1942–8. 4.
[41] Minh HL, Khatir S, Rao RV. A variable velocity strategy particle swarm optimization algorithm (VVS-PSO) for damage assessment in structures. Eng Comput 2021:1–30.
[42] Minh HL, Khatir S, Wahab MA. An enhancing particle swarm optimization algorithm (EHVPSO) for damage identification in 3D transmission tower. Eng Struct 2021;242:112412.
[43] Tran-Ngoc H, He L, Reynders E, et al. An efficient approach to model updating for a multispan railway bridge using orthogonal diagonalization combined with improved particle swarm optimization. J Sound Vib 2020;476:115315.
[44] Fahimi N, Sezavar HR, Akmal AAS. Dynamic modeling of flashover of polymer insulators under polluted conditions based on HGA-PSO algorithm. Electric Power Syst Res 2022;205:107728.
[45] Politis S N, Colombo P, Colombo G, et al. Design of experiments (DoE) in pharmaceutical development. Drug Dev Ind Pharm 2017;43(6):889–901.
[46] Chicco D, Warrens MJ, Jurman G. The coefficient of determination R-squared is more informative than SMAPE, MAE, MAPE, MSE and RMSE in regression analysis evaluation. PeerJ Comp Sci 2021;7:e623.
[47] Shi B, Qiao P. A new surface fractal dimension for displacement mode shape-based damage identification of plate-type structures. Mech Syst Signal Process 2018;103: 139–61.
[48] Diaz P, Doostan A, Hampton J. Sparse polynomial chaos expansions via compressed sensing and D-optimal design. Comput Methods Appl Mech Eng 2018; 336:640–66.
[49] Lin DKJ, Simpson TW, Chen W. Sampling strategies for computer experiments: design and analysis. Int J Reliab Appl 2001;2(3):209–40.
[50] ANSYS, Ansys software reference manuals, release notes, mechanical APDL, elements reference, commands reference and theory reference, version release 18, 2017.
[51] Marelli S, Sudret B. UQLab: a framework for uncertainty quantification in matlab. American Society of Civil Engineers; 2014 [M].
[52] Wei Q, Shen L, Cao M, et al. A novel method for identifying damage in transverse joints of arch dams from seismic responses based on the feature of local dynamic continuity interruption. Smart Mater Struct 2023.